Post-tetanic increase in the fast-releasing synaptic vesicle pool at the expense of the slowly releasing pool

Jae Sung Lee, Won-Kyung Ho, and Suk-Ho Lee

Department of Physiology and Biomembrane Plasticity Research Center, Seoul National University College of Medicine and Neuroscience Research Institute, Seoul, 110-799, Korea

Post-tetanic potentiation (PTP) at the calyx of Held synapse is caused by increases not only in release probability (P_r) but also in the readily releasable pool size estimated from a cumulative plot of excitatory post-synaptic current amplitudes (RRP_{cum}), which contribute to the augmentation phase and the late phase of PTP, respectively. The vesicle pool dynamics underlying the latter has not been investigated, because PTP is abolished by presynaptic whole-cell patch clamp. We found that supplement of recombinant calmodulin to the presynaptic pipette solution rescued the increase in the RRP_{cum} after high-frequency stimulation (100 Hz for 4-s duration, HFS), but not the increase in P_r. Release-competent synaptic vesicles (SVs) are heterogeneous in their releasing kinetics. To investigate post-tetanic changes of fast and slowly releasing SV pool (FRP and SRP) sizes, we estimated quantal release rates before and 40 s after HFS using the deconvolution method. After HFS, the FRP size increased by 19.1% and the SRP size decreased by 25.4%, whereas the sum of FRP and SRP sizes did not increase. Similar changes in the RRP were induced by a single long depolarizing pulse (100 ms). The post-tetanic complementary changes of FRP and SRP sizes were abolished by inhibitors of myosin II or myosin light chain kinase. The post-tetanic increase in the FRP size coupled to a decrease in the SRP size provides the first line of evidence for the idea that a slowly releasing SV can be converted to a fast releasing one.

INTRODUCTION

Post-tetanic potentiation (PTP) results from a presynaptic enhancement of synaptic vesicle (SV) release, which lasts for tens of seconds after a cessation of tetanic stimulation. Although the peak magnitude of PTP primarily depends on the increase in release probability (P_r) caused by post-tetanic residual calcium (Korogod et al., 2005), the increase in the readily releasable pool (RRP) size lasts longer than that in P_r at the calyx of Held synapse (Habets and Borst, 2007; Lee et al., 2008). Moreover, the overall decay time course of PTP is dominated by that of the RRP size at physiological temperature, because the RRP enlargement becomes more significant while the decay of P_r becomes faster (Habets and Borst, 2007). Therefore, study of synaptic vesicle dynamics underlying the post-tetanic changes in RRP is essential for understanding the late phase of PTP.

Previous studies have estimated the post-tetanic change in the RRP size from a cumulative plot of excitatory post-synaptic current (EPSC) amplitudes evoked by a train of high-frequency stimuli (Schneggenburger et al., 2002; Habets and Borst, 2005, 2007; Lee et al., 2008). An estimate of the RRP size is essential for quantitative analysis of presynaptic plasticity, but heavily depends on the way of measurement. During the last decade, the deconvolution method rigorously proved the previous notion that P_r of SVs in the RRP is heterogeneous at the calyx of Held (Wu and Borst, 1999), and revealed that the RRP can be separated into fast and slow releasing pools (FRP and SRP), which are distinct with respect to P_r and recruitment speed (Neher and Sakaba, 2001; Sakaba and Neher, 2001a). Only a part of the RRP, mainly FRP, comprises the RRP size measured by a cumulative EPSC plot (RRP_{cum}) (Sakaba, 2006). In general, RRP_{cum} seems to be the most parsimonious way for estimation of release-competent (or docked) SVs at a glutamatergic synapse, considering that RRP_{cum} is about a fifth of the RRP size reported by hypertonic sucrose method in the hippocampal neuron (Moulder and Mennerick, 2005). These discrepancies prompted us to study post-tetanic changes in the RRP size in a different way other than a cumulative EPSC plots. Therefore, using the deconvolution method, we tried to address

Correspondence to Suk-Ho Lee: leesukho@snu.ac.kr

Abbreviations used in this paper: aCSF, artificial cerebrospinal fluid; AFS, afferent fiber stimulation; AP, action potential; $[Ca^{2+}]_{pre}$, presynaptic intracellular $[Ca^{2+}]$; CaM, calmodulin; CaT, Ca^{2+} transients; γ-DGG, γ-D-glutamylglycine; EPSC, excitatory post-synaptic current; FRP, fast releasing synaptic vesicle pool; HFS, high frequency stimuli; ISI, inter stimulus interval; mEPSC, miniature EPSC; MLCK, myosin light chain kinase; MLCKip, MLCK inhibitor peptide-18; PPR, paired-pulse ratio; P_r, release probability; PT, physiological temperature; PTP, post-tetanic potentiation; RRP, readily releasable pool; RRP_{cum}, RRP size measured by a cumulative EPSC plot; RT, room temperature; SRP, slowly releasing synaptic vesicle pool; SV, synaptic vesicle; WCR, whole-cell patch recording.

The Rockefeller University Press $30.00
J. Gen. Physiol. Vol. 136 No. 3 259–272
www.jgp.org/cgi/doi/10.1085/jgp.201010437

the question of whether PTP is associated with an increase of only FRP size or total RRP size.

Investigation of SV dynamics underlying PTP using the deconvolution method has been hindered because whole-cell patch recording (WCR) of the presynaptic terminal necessary to use the deconvolution method prevents PTP due to unknown reasons, probably due to dilution of essential intracellular components (Korogod et al., 2005). Previously, we have reported that post-tetanic increase in the RRP_{cum} size is mediated by a mechanism involving calmodulin (CaM) and myosin light chain kinase (MLCK), independent of residual calcium level ($\Delta[Ca^{2+}]$), which mediates the post-tetanic increase in P_r (Lee et al., 2008). Implied by our previous findings, we hypothesized that dilution of intracellular CaM with a patch pipette solution may be one of the reasons for the lack of PTP during presynaptic WCR, and found that presynaptic supplement of recombinant CaM rescues the post-tetanic increase in the RRP_{cum} size. Further investigation using the deconvolution method revealed that not only tetanic stimulation but also a single strong depolarization increase the FRP size at the expense of the SRP size with no significant change of the total RRP size, indicative of conversion of a slowly releasing SV into a fast releasing one (Neher and Sakaba, 2008).

MATERIALS AND METHODS

Brain stem preparation and solutions

Transverse 200–250-μm-thick brain stem slices containing the medial nucleus of trapezoid body were prepared from 7- to 9-day-old Sprague Dawley rats as previously described (Kim et al., 2005). Protocols were approved by the Animal Care Committee at Seoul National University. The brain stem obtained from a rat was chilled in ice-cold low-calcium artificial cerebrospinal fluid (aCSF) containing (in mM) 125 NaCl, 25 $NaHCO_3$, 2.5 KCl, 1.25 NaH_2PO_4, 2.5 $MgCl_2$, 0.5 $CaCl_2$, 25 glucose, 0.4 Na ascorbate, 3 myoinositol, and 2 Na pyruvate (pH, 7.4 when saturated with carbogen [95% O_2, 5% CO_2]; osmolarity, ~320 mOsm). After making brain stem slices, they were incubated at 37°C for 30 min in normal aCSF, the constituents of which were the same as low-calcium aCSF except 1 mM $MgCl_2$ and 2 mM $CaCl_2$, and thereafter maintained at room temperature (RT, 23–25°C) until required.

Electrophysiological recording and reagents

Slices were transferred to a recording chamber in an upright microscope (BX50WI; Olympus). In most experiments (except in Fig. 1), 1 μM tetrodotoxin, 50 μM D-AP5, and 10 mM TEA-Cl were added to the bath solution to isolate presynaptic Ca^{2+} current and AMPA receptor-mediated EPSC. Moreover, 100 μM cyclothiazide and 2 mM γ-D-glutamylglycine (γ-DGG) were added to prevent desensitization and saturation of AMPA receptors, respectively. 2 mM γ-DGG reduced the EPSC amplitude to a half of the control value. A presynaptic terminal and the postsynaptic medial nucleus of trapezoid body neurons were simultaneously whole-cell clamped at −80 mV and −70 mV, respectively. The postsynaptic pipette (3–4 MΩ) solution (in mM) contained 130 cesium-gluconate, 20 TEA-Cl, 10 NaCl, 20 HEPES, 5, sodium-phosphocreatine, 4 Mg-ATP, and 10 EGTA with pH adjusted at 7.3. The presynaptic patch pipette (4–5 MΩ) solution contained (in mM) 130 cesium-gluconate, 20 TEA-Cl, 20 HEPES, 5 sodium-phosphocreatine, 4 Mg-ATP, 0.3 Na-GTP, and 0.5 EGTA (0.2 mM in Fig. 1 and Fig. S2) with pH adjusted at 7.3 using CsOH. The presynaptic series resistance (R_s, 10–25 MΩ) was compensated by 50–80%, and the postsynaptic series resistance (4–15 MΩ) was compensated by up to 70%, such that remaining uncompensated R_s values were 5 MΩ and 3–4 MΩ for pre- and postsynaptic pipettes, respectively. The remaining postsynaptic resistance was further compensated offline. Recordings were made at room temperature (23–25°C) with an EPC10/2 amplifier (HEKA). A presynaptic action potential was emulated by an action potential (AP)–like ramp pulse, which consists of an upstroke phase from −80 to +40 mV over 0.4 ms followed by a depolarization phase to −80 mV over 0.8 ms. PTP of EPSC was quantified as ([EPSC2–EPSC1]/EPSC1) x 100 (%), where EPSC1 and EPSC2 are EPSC amplitudes before and after high-frequency stimuli (HFS), respectively. Most of experiments in this study were done with recombinant CaM included in the presynaptic patch pipette. By taking into account molecular weight of CaM (97 KD) and typical values for series resistance (15 MΩ) and volume of the calyx terminal (0.48 pL; Sätzler et al., 2002), the time constant for diffusion of CaM out of the patch pipette is calculated to be 104 s based on the empirical formula of Pusch and Neher (1988). Typically, we started to study PTP ~500 s after establishing WCR, which is long sufficient for CaM in the patch pipette to be equilibrated with the cytosol, although the diffusion time constant may be longer than the calculated value owing to the finger-like structure of calyx terminals. Recombinant CaM was purchased from Jena Bioscience; tetrodotoxin, DL-AP5, cyclothiazide, and γ-DGG were purchased from Tocris. Myosin light chain kinase inhibitor peptide 18 (MLCKip) was obtained from EMD. Wortmannin and blebbistatin were from Biomol.

The deconvolution method

Quantal release rates were estimated using the deconvolution method, which corrects delayed glutamate clearance component of synaptic cleft at the calyx of Held synapse (Neher and Sakaba, 2001). We applied "fitting protocols" to determine parameters of glutamate diffusion model at the start of each experiment (exemplary traces and fitting parameters are shown in Fig. S1). The criteria for an appropriate parameter set were as follows. (1) Residual current was small or absent after the first pulse of fitting protocol. (2) No negative release rate occurred during a whole trace. (3) At times after stimulation, no transmitter release was expected and release rate should be 0 between stimulation episodes. After determination of the parameters for a given synapse, we used the same parameters for other traces within the same cell pair. Cumulative release was obtained from the integration of release rate traces and fitted with double-exponential function.

Presynaptic $[Ca^{2+}]$ imaging

Presynaptic Ca^{2+} concentrations during and after HFS were measured by fluorescence imaging. The constituents of the pipette solution were the same as the standard presynaptic patch pipette solution except that 0.5 mM EGTA was replaced with 0.4 mM EGTA and 0.1 mM fura-4F. The excitation light from a monochromator (Polychrome-IV; TILL Photonics) was delivered to the upright microscope via a quartz light guide and a built-in condenser. Imaging was performed using a 60x water immersion objective (NA, 0.9; LUMPlanFl; Olympus) and an air-cooled slow-scan CCD camera (SensiCam; PCO) using on-chip binning (8 × 16 pixels). The fluorescence ratio ($R = F_{iso}/F_{380}$) at the isosbestic wavelength (360 nm; F_{iso}) to that at 380 nm (F_{380}) was converted to $[Ca^{2+}]_i$ according to the following equation:

$$[Ca^{2+}]_i = K_{eff} \bullet (R - R_{min}) / (R_{max} - R).$$

Calibration parameters were determined by "in-cell" calibration. R_{min} value was measured using a Ca^{2+}-free internal solution containing 10 mM BAPTA. R_{max} value was obtained from in vitro measurement, because calyces of Held did not endure internal dialysis with high $CaCl_2$ (10 mM). The calibration ratio at intermediate $[Ca^{2+}]_i$ (R_{int}) was measured in the calyx using a pipette solution containing 8 mM BAPTA and 6 mM $CaCl_2$ ($[Ca^{2+}]_i \approx 660$ nM) for fura-4F. The effective dissociation constant of fura-4F (K_{eff}) was calculated by rearranging the equation above for K_{eff} after inserting R_{int} and the intermediate $[Ca^{2+}]_i$ values. The K_d values of fura-4F were calculated as 0.74 µM from $K_d = K_{eff} \cdot (\alpha + R_{min})/(\alpha + R_{max})$, where α is the isosbestic coefficient.

Data analysis

Data were analyzed using IgorPro (version 4.1; WaveMetrics). Statistical data are expressed as mean ± SEM, and *n* indicates the number of synapses studied. Unless mentioned otherwise, the first and the second statistical values in a parenthesis intervened by "vs." represent statistical data under test conditions and under control conditions, respectively. Statistical analyses on data obtained from the same synapse and those on data from different synapses were performed using Student's paired *t* test and the Student's *t* test, respectively. Statistical significance was determined with a threshold P value of 0.05 (*) or 0.01 (**). For simplicity, some statistical data with no significant difference were not shown in the text, but shown in Table S1.

Online supplemental materials

Table S1 contains all statistical values of this paper. Fig. S1 shows an exemplary trace for the fitting protocol. Fig. S2 contains parameters for baseline synaptic strength under the experimental conditions of Fig. 1. Fig. S3 demonstrates no change in the distribution of miniature EPSC (mEPSC) after tetanic stimulation. Fig. S4 shows the changes of FRP and SRP sizes during PTP by using a paired pulse protocol. Fig. S5 illustrates no post-tetanic change in the RRP size without CaM. Fig. S6 and S7 show that wortmannin (Fig. S6) or blebbistatin (Fig. S7) suppresses the post-tetanic RRP changes induced by tetanic stimulation. Fig. S8 shows no effect of a single 50 ms depolarization pulse on the vesicle dynamics. Fig. S9 depicts bar graphs which summarize releasing time constants. The online supplemental material is available at http://www.jgp.org/cgi/content/full/jgp.201010437/DC1.

RESULTS

Presynaptic supplement of recombinant CaM rescues post-tetanic increase in the RRP_{cum} size during presynaptic whole-cell recording

PTP involves increases both in P_r and the RRP size estimated from the plots of cumulative EPSC amplitude (RRP_{cum}) (Habets and Borst, 2005, 2007; Lee et al., 2008). Presynaptic WCR abolishes PTP at the calyx of Held synapse (Korogod et al., 2005). We confirmed this effect of presynaptic WCR on PTP, and found that WCR abolished not only post-tetanic increase in P_r but also the increase in RRP_{cum} size (Fig. 1 A). Little increase in P_r can be explained by the previous findings that presynaptic WCR reduces post-tetanic residual calcium (Korogod et al., 2005) and the post-tetanic increase in P_r is proportional to residual $\Delta[Ca^{2+}]$ (Lee et al., 2008). The lack of increase in the RRP_{cum} size, however, cannot be explained by the reduced residual calcium because the post-tetanic increase in the RRP_{cum} size is regulated by a mechanism involving CaM and MLCK, independent of residual calcium (Lee et al., 2008). Implied by our previous results, we hypothesized that the lack of post-tetanic RRP_{cum} change under WCR conditions is caused by washout of intracellular CaM through the patch pipette.

To test this hypothesis, we performed dual WCR at the calyx of Held synapse and monitored PTP of EPSCs evoked by a pair of AP-like ramp pulses (inter-stimulus interval [ISI], 20 ms) given to the presynaptic terminal at 0.1 Hz via a presynaptic patch pipette, in which 3 µM recombinant CaM was supplemented. To prevent saturation and desensitization of post-synaptic AMPA receptors, EPSCs were recorded in the presence of 4 mM γ-DGG in aCSF, and 0.2 mM EGTA was included in the presynaptic patch pipette to mimic physiological buffer concentration (Borst and Sakmann, 1996). After assessment of baseline EPSCs (0.74 ± 0.15 nA, $n = 5$), we applied HFS of AP-like pulses at 100 Hz for 4 s, and then resumed the paired pulse to monitor PTP. In the presence of recombinant CaM, the magnitude of PTP was significantly higher (66.1 ± 14.0%, $n = 6$; Fig. 1, B, a, and C) than that without CaM (8.2 ± 10.0%, $n = 5$; Fig. 1, A, a, and C), but lower than PTP induced by afferent fiber stimulation (AFS) without presynaptic WCR (128%; Lee et al., 2008). PTP accompanied increases both in the RRP_{cum} size and in P_r. The increment in the RRP_{cum} size was not different from that estimated in AFS experiments (27.4 ± 8.2%, $n = 6$, vs. 19.3 ± 2.5%, $n = 11$, $P = 0.25$), indicating that presynaptic supplement of CaM rescues the post-tetanic increase of the RRP_{cum} size (Fig. 1 D). In contrast, the post-tetanic increase in P_r was significantly lower than that estimated in AFS experiments (35.1 ± 7.6%, $n = 6$, vs. 95.4 ± 13.4%, $n = 11$, $P < 0.01$), and rather similar to that measured in AFS experiments when mitochondria-derived residual calcium was blocked by 2 µM tetraphenylphosphonium (TPP), a blocker of mitochondrial Na/Ca exchanger (45.9 ± 7.7%, $n = 6$, $P = 0.34$; Fig. 1 E; Lee et al., 2008). Moreover, the post-tetanic increments in P_r were not different regardless of presynaptic CaM supplement under dual WCR conditions ($P = 0.16$; Fig. 1 E). Accordingly, no significant change in paired-pulse ratio (PPR, $EPSC_2/EPSC_1$; ISI, 20 ms) was observed under dual WCR conditions ($P > 0.05$, paired *t* test; Fig. 1 F), whereas PPR was significantly reduced during PTP induced by AFS without TPP ($P < 0.01$, paired *t* test). These results indicate that dilution of CaM in the presynaptic terminal by the patch pipette solution is responsible for the WCR-induced suppression of post-tetanic increase in the RRP_{cum} size, but not for P_r. The basal EPSC amplitude, the RRP size, and P_r were not different among all groups (Fig. S2).

Tetanic stimulation increases the FRP size at the expense of the SRP size

The RRP_{cum} size represents a part of total RRP estimated by a presynaptic long depolarization (Sakaba, 2006).

To examine post-tetanic changes in the size and release kinetics of the RRP during PTP, we calculated quantal release rate from EPSCs evoked by a long depolarization before and after HFS by using the deconvolution methods (Neher and Sakaba, 2001). For clear separation of two components of RRP, we raised [EGTA] to 0.5 mM in the presynaptic patch pipette solution (Sakaba and Neher, 2001a). We recorded EPSCs evoked by a presynaptic long depolarization pulse (50 ms) at 40 s before and after the HFS (AP-like pulses at 100 Hz for 4 s) in order for the RRP to be fully recovered from depletion, and recorded another EPSC at 120 s after the HFS, at which post-tetanic effects are supposed to be subsided (Fig. 2 A). When 3 μM CaM was included in the presynaptic patch pipette, HFS significantly increased the EPSC amplitude at 40 s after HFS by 10.4 ± 1.5% (18.8 nA ± 2.0 nA to 20.6 ± 2.1 nA, $n = 9$, $P < 0.01$, paired t test), but no significant change in presynaptic Ca^{2+} current was observed (Fig. 2, B, D, and F). Intriguingly, HFS had significant effects not only on the amplitude

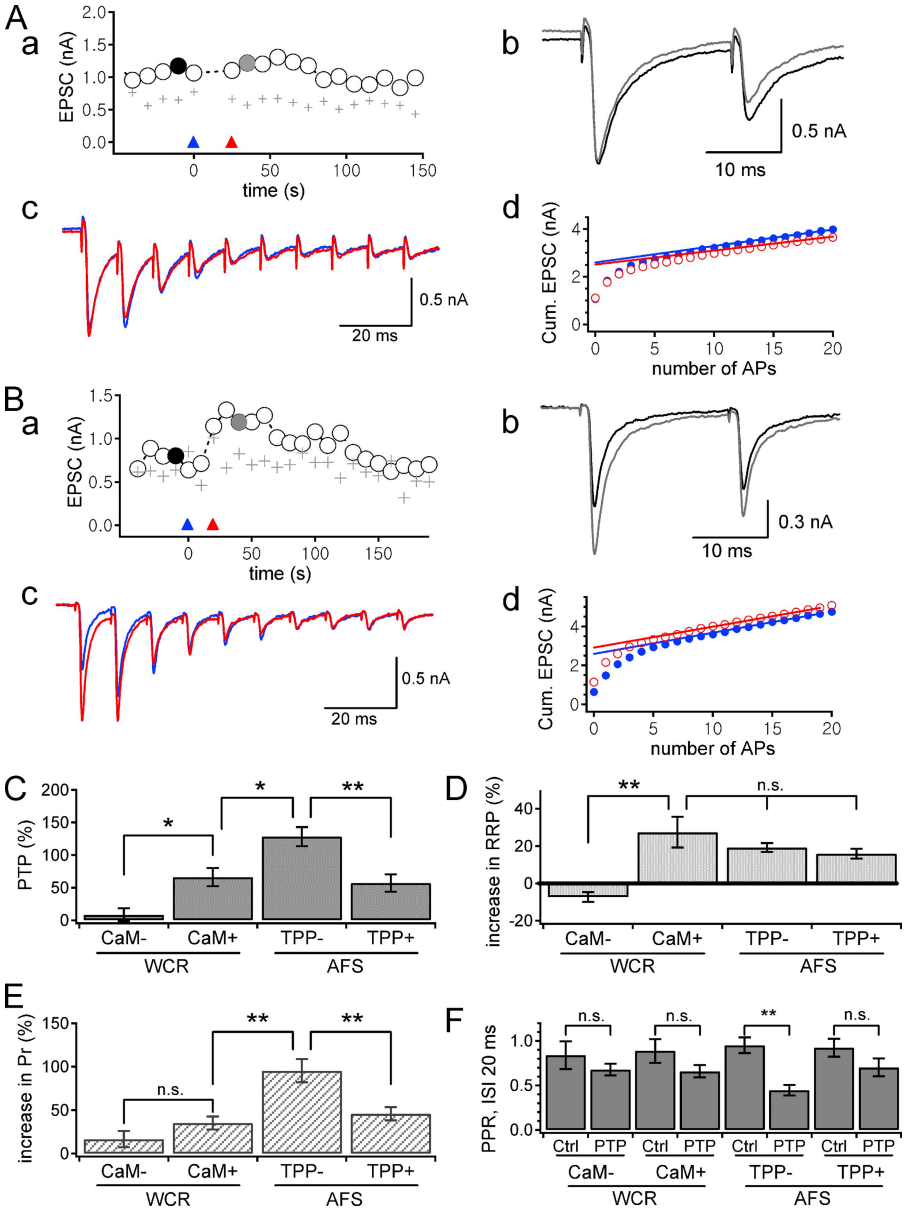

Figure 1. Induction of PTP using dual whole-cell patch recordings (WCR) at calyx of Held synapses with presynaptic pipette solution free of CaM (A) or supplemented with CaM (B). (A, a) A time course of EPSC amplitudes evoked by a paired AP-like pulses applied to the presynaptic terminal every 10 s. Open circles and gray crosses are the first and the second EPSC amplitudes to paired pulses (inter-stimulus interval, 20 ms), respectively. Blue and red triangles indicate the time points when HFS (a train of AP-like ramp pulses at 100 Hz for 4 s) and a short train of 20 pulses at 100 Hz were applied. (A, b) EPSCs recorded at black and gray filled circles in A (a) are superimposed. (A, c) First 10 EPSCs evoked by HFS (blue) and a short train of 20 pulses at 100 Hz (red) are superimposed. (A, d) Plots of cumulative (cum.) EPSC amplitude evoked by HFS (blue circles) and a short train of pulses (red circles) shown in A (c). The RRP size was estimated at the y intercept of the back extrapolation line fitted to the last five points. Release probability (P_r) was estimated from the first EPSC amplitude divided by the estimate of the RRP size (RRP_{cum}). (B, a–d) The same experiment as in A (a–d) at a different synapse except supplement of 3 μM recombinant CaM in the presynaptic pipette solution. The symbols and scheme are the same as in A (a–d). (C–E) Mean values for PTP (C), increments in the RRP size (D), and P_r (E) measured at 20 s after HFS under the following conditions: dual whole-cell patch recordings without (WCR and CaM−) or with supplement of 3 μM CaM in the presynaptic pipette solution (WCR and CaM+) and afferent axon fiber stimulation (AFS and TPP−) in control or in the presence of 2 μM tetraphenylphosphonium (TPP) in the bath solution (AFS and TPP+). (F) Average paired-pulse ratio (PPR; inter-stimulus interval, ISI = 20 ms) before HFS (Ctrl) and at the peak of PTP (PTP). Mean ± SEM; *, $P < 0.05$; **, $P < 0.01$ (unpaired t test for C–E, paired t test for F).

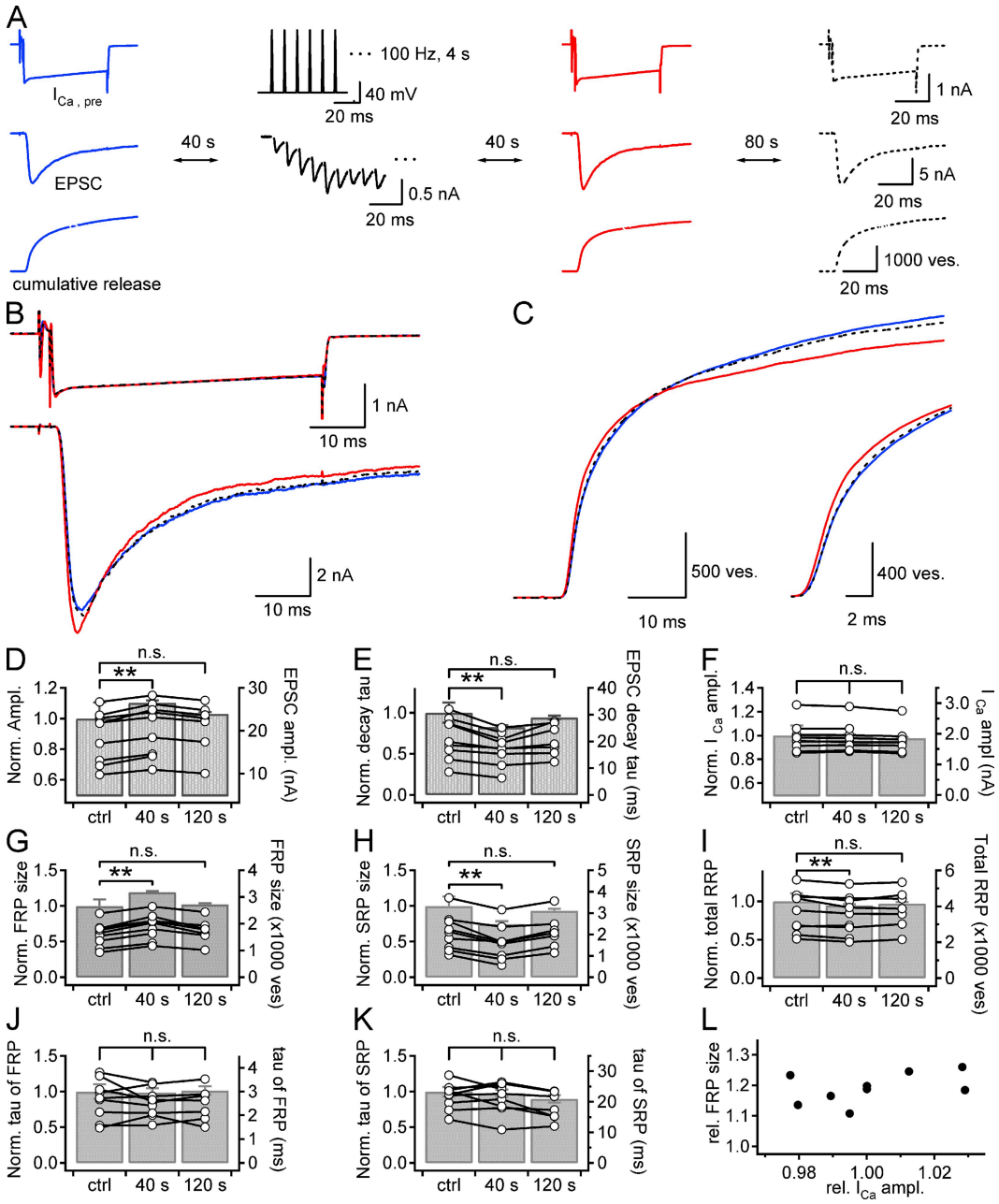

Figure 2. Post-tetanic increase in the FRP size at the expense of the SRP size. (A) Simultaneous recordings of presynaptic Ca^{2+} current ($I_{Ca,pre}$; top), EPSC (middle), and cumulative quantal release (bottom) are shown in a chronological order: 40 s before HFS (a train of AP-like pulses at 100 Hz for 4 s) and 40 s and 120 s after HFS. $I_{Ca,pre}$ was evoked by a long depolarization pulse to 0 mV for 50 ms preceded by a predepolarization to +70 mV for 2 ms to ensure fast activation of presynaptic Ca^{2+} current. The second column shows EPSC (bottom) in response to HFS, a train of AP-like ramp pulses for 4 s at 100 Hz applied to presynaptic terminal (top). B and C show presynaptic Ca^{2+} currents (B, top), EPSCs (B, bottom), and cumulative quantal release (C). Each panel illustrates three superimposed traces recorded before HFS (blue solid line) and 40 s (red solid line) and 120 s (broken line) after HFS in the same synapse as in A. (C, inset) Cumulative quantal release on an expanded time scale. (D–K) Bar graphs illustrate statistical mean of relative values before (ctrl) and after HFS (40 s and 120 s) normalized to the control value measured before HFS. (D) EPSC amplitude; (E) decaying time constant of EPSC; (F) amplitude of $I_{Ca,pre}$; (G) size of the FRP; (H) size of the SRP; (I) size of total RRP; (J) release time constant (τ) of the FRP; (K) release τ of the SRP. Data of individual synapses are shown as circles connected with a line superimposed on the bar graph (right ordinate). Error bar, SEM; *, $P < 0.05$; **, $P < 0.01$; n.s., not significant ($P > 0.05$, paired *t* test). (L) Plot of the relative post-tetanic FRP size as a function of the relative post-tetanic amplitude of presynaptic Ca^{2+} current ($I_{Ca,pre}$) normalized to control values measured before HFS ($n = 9$).

but also on the decaying kinetics of post-tetanic EPSC. The decay time constant (τ) of EPSC became significantly faster at 40 s after HFS (21.2 ± 2.6 ms to 17.4 ± 2.0 ms, $n = 9$, $P < 0.01$, paired t test) (Fig. 2, B and E). In seven out of nine synapses, we could evoke another EPSC by the same depolarization pulse at 120 s after HFS, and found that these post-tetanic changes of EPSC disappeared. At this time point, the amplitude of EPSC and decay τ of EPSC returned to the control level (Fig. 2, B, D, and E; Table S1).

Heterogeneity in release kinetics of docked vesicle pools can be resolved by applying the deconvolution method to EPSC trace evoked by a long depolarization in the presence of 0.5 mM EGTA (Sakaba and Neher, 2001a). The quantal release rate was calculated using a set of parameters determined from a fitting-protocol at a given synapse. We assumed that the quantal size does not change after HFS under our experimental conditions because cumulative mEPSC amplitude distribution was identical before and after HFS (Fig. S3). Calculation of quantal release rates revealed that the FRP size significantly increased at 40 s after HFS (1602 ± 147 to 1896 ± 158 vesicles [ves], 119.1 ± 1.7% of control, $n = 9$, $P < 0.01$, paired t test; Fig. 2 G). The increase in the FRP size was accompanied by a significant decrease in the SRP size (2099 ± 280 to 1613 ± 264 ves, 74.6 ± 4.1% of control, $n = 9$, $P < 0.01$, paired t test; Fig. 2 H). These changes were no longer observed at 120 s after HFS. Sizes of the FRP and the SRP returned to 102.2 ± 1.4% and 93.3 ± 3.0% of control value, respectively ($n = 7$, $P = 0.15$ and 0.06, paired t test). The estimate for the total RRP size at 40 s after HFS was rather slightly reduced to 94.8 ± 1.3% of control ($n = 9$, $P < 0.01$, paired t test), indicating that the FRP increase is not caused by an increase in the total RRP size. At 120 s after HFS, the total RRP size was recovered close to the control size (96.9 ± 1.9% of control, $n = 7$, $P = 0.14$, paired t test) (Fig. 2 I). The amplitudes of presynaptic Ca^{2+} current ($I_{Ca,pre}$) were not different among the three time points (Fig. 2 F, Table S1). The amplitudes of presynaptic calcium current ($I_{Ca,pre}$) were not always identical before and after HFS, but, if any, the variance of $I_{Ca,pre}$ amplitude was not large enough to cause a correlative change of the FRP size (Fig. 2 L), indicating that the effect of post-tetanic change of $I_{Ca,pre}$ is negligible. The fast and slow time constants for SV release (fast and slow release τ) were not significantly different at all time points (Fig. 2, J and K).

As a substitute for the deconvolution methods, we tried to split EPSCs contributed by release of SVs in FRP and SRP using a paired-pulse protocol. Because the EPSC amplitude stayed constant with presyanptic depolarization longer than 5 ms, the first pulse (5 ms in duration) for depletion of FRP was followed by the second pulse (30 ms in duration) for depletion of SRP with ISI of 15 ms (Fig. S4 A). During PTP (at 40 s after HFS), the first EPSC amplitude was significantly increased, while the second EPSC was decreased (Fig. S4, C, F, and G). These changes recovered at 120 s after HFS. The opposite change in the amplitude of first and second EPSCs is consistent with the results of deconvolution analysis.

When CaM was omitted from the presynaptic pipette solution, the same HFS did not change the amplitude and decay kinetics of EPSC at 40 s after HFS (Fig. S5). Consequently, no significant change was found in the FRP and SRP sizes, indicating that the post-tetanic increase in the FRP size depends on presynaptic CaM, but not on presynaptic residual calcium. For unknown

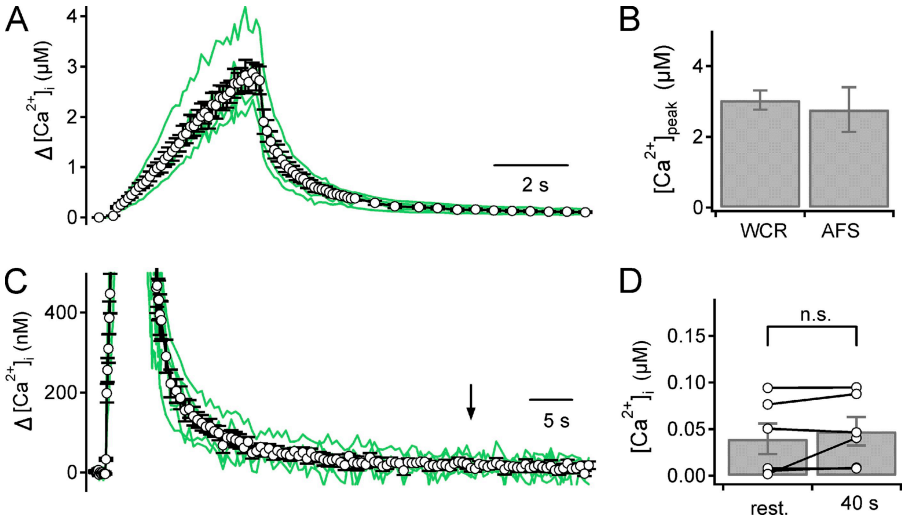

Figure 3. (A) Ca^{2+} transients (CaTs) evoked by a train of AP-like ramp pulses at 100 Hz for 4 s (HFS). CaTs recorded at 6 synapses (green lines) and an averaged $\Delta[Ca^{2+}]_i$ trace (open circles with error bars) are superimposed. Presynaptic $[Ca^{2+}]_i$ during and after HFS were measured by fluorescence imaging the presynaptic terminal loaded with 100 μM Fura-4F via a patch pipette. (B) The mean peak value of $\Delta[Ca^{2+}]_i$ evoked by HFS measured using dual WCR (3.04 ± 0.27 μM, $n = 6$) is compared with that evoked by AFS at 100 Hz for 4 s (2.77 ± 0.63 μM, $n = 5$). (C) CaTs are the same as in A but on expanded scales of time and $\Delta[Ca^{2+}]_i$. (D) Mean values for resting $[Ca^{2+}]_i$ before and 40 s after HFS (39.5 ± 16.4 nM and 47.8 ± 15.3 nM, respectively, $n = 6$, $P = 0.25$, paired t test). The black arrow in C indicates the time point of 40 s after HFS. Mean ± SEM; n.s., not significant ($P > 0.05$, paired t test).

reasons, release time constant of the FRP was significantly slowed at 40 s after HFS (1.77 ± 0.22 ms vs. 1.42 ± 0.13 ms, $n = 5$, P = 0.04, paired t test; Fig. S5 J), which is contrasted with no change in release time constants after HFS in the presence of CaM ($n = 10$, P = 0.47, paired t test; Fig. 2 J).

Post-tetanic increase in the FRP size cannot be ascribed to residual calcium

Previous results indicate that post-tetanic increase in the RRP_{cum} size is not caused by residual calcium but by the $[Ca^{2+}]_i$ elevation during HFS (Lee et al., 2008). We tested whether the peak presynaptic $[Ca^{2+}]_i$ ($[Ca^{2+}]_{pre}$) attained by a train of AP-like pulses via a whole-cell patch pipette is comparable to that by AFS reported in our previous study (Lee et al., 2008). Presynaptic Ca^{2+} transients (CaTs) were recorded with a presynaptic pipette solution containing 0.4 mM EGTA and 0.1 mM fura-4F instead of 0.5 mM EGTA. As expected from the presence of high calcium buffer, the rising phase of the CaT was slower than that evoked by AFS, but the peak $[Ca^{2+}]_{pre}$ was not different from that evoked by AFS in our previous study (3.0 ± 0.3 μM, $n = 6$, vs. 2.8 ± 0.6 μM, $n = 5$, P = 0.68; Fig. 3, A and B). Moreover, in agreement with the previous result that presynaptic WCR largely abolished residual calcium after HFS (Korogod et al., 2005), the $[Ca^{2+}]_{pre}$ at 40 s after HFS was not different from the resting $[Ca^{2+}]_{pre}$ ($n = 6$, P = 0.25, paired t test; Fig. 3, C and D).

Post-tetanic increase in the FRP size is abolished by MLCK inhibitor peptide or blebbistatin

Previously, we have reported that post-tetanic increase in the RRP_{cum} size is abolished by inhibitors of MLCK and myosin II ATPase (Lee et al., 2008). We tested the effects of these inhibitors on post-tetanic increase in the FRP size. When 10 μM MLCK inhibitory peptide-18 (MLCKip) was added to the presynaptic patch pipette together with 3 μM CaM, EPSC amplitude did not increase at 40 s after HFS (16.0 ± 2.5 nA vs. 16.3 ± 2.4 nA, $n = 6$, P = 0.11, paired t test) as well as at 120 s after HFS (Fig. 4, A and C). The decay τ of EPSC did not change either at 40 s after HFS (21.6 ± 3.7 ms vs. 20.2 ± 3.5 ms, $n = 6$, P = 0.21, paired t test) and at 120 s after HFS (Fig. 4, A and D). Consequently, we found no significant change in estimates for the FRP size, SRP size, and releasing

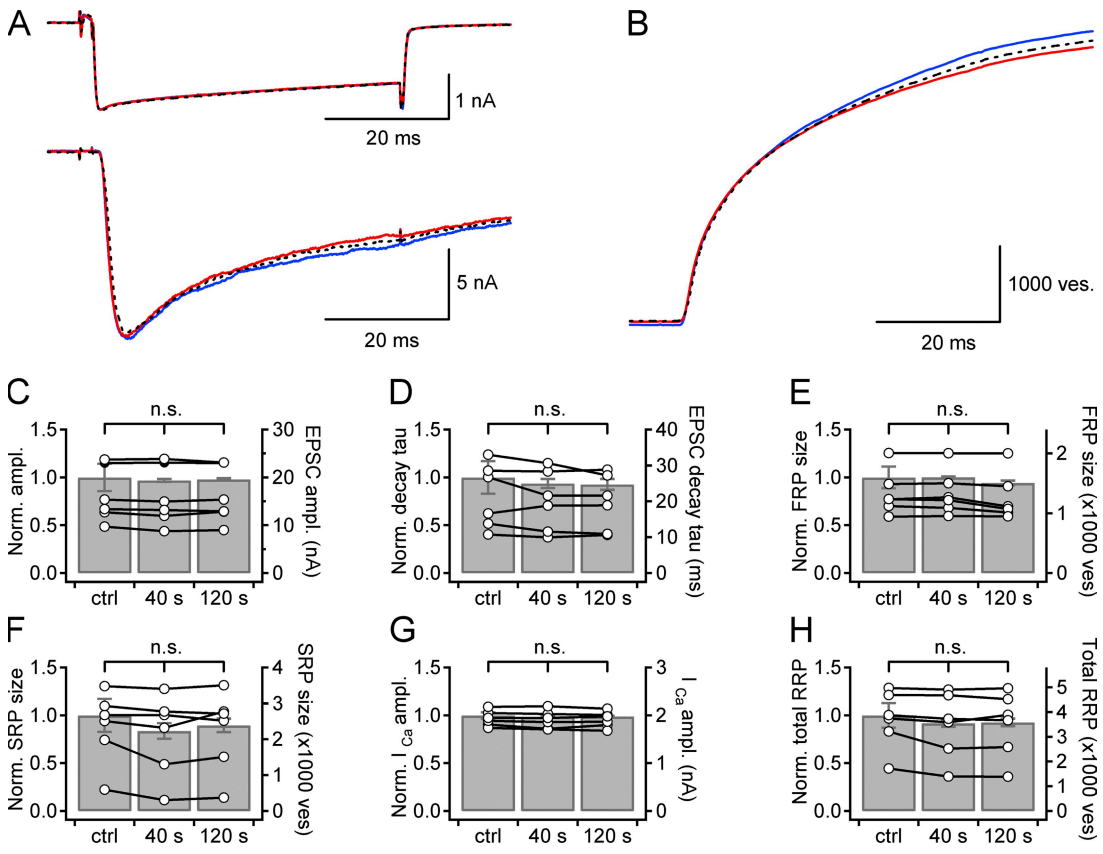

Figure 4. MLCK inhibitor peptide-18 (MLCKip) suppresses the post-tetanic changes in FRP and SRP sizes. (A and B) Presynaptic Ca^{2+} current (A, top), EPSCs (A, bottom) and cumulative quantal release (B). Three traces are superimposed in each panel: recordings at 40 s before (blue solid line) and at 40 s (red solid line) and 120 s (broken line) after HFS. (C–H) Bar graphs illustrate statistical mean of relative values at different time points normalized to the control value measured before HFS. Data from an individual synapse are superimposed on the bar graph (open circles, right ordinate). Error bar, SEM; n.s., not significant (P > 0.05, paired t test).

time constants (Fig. 4, E–H; Table S1). Because ML-7, an MLCK inhibitor, has been reported to have off-target effects on calcium current and synaptic transmission, we tested another MLCK inhibitor, wortmannin, which has reportedly no effect on the calcium current (Tokuoka and Goda, 2006). In addition, we tested the effects of blebbistatin, a myosin II ATPase inhibitor. Similar to MLCKip, presynaptic treatment of 3 µM wortmannin or 100 µM blebbistatin together with 3 µM CaM suppressed the post-tetanic changes in EPSC, the FRP size and the SRP size that were observed in the presence of CaM only (Fig. S6 for wortmannin; Fig. S7 for blebbistatin; Table S1). These results suggest that the post-tetanic increase in the RRP_{cum} size and the increase in the FRP size at the expense of SRP share the common underlying mechanism, which probably involves MLCK and myosin II (Lee et al., 2008). The SRP size marginally decreased at 40 s after HFS (P = 0.06, $n = 6$; P = 0.08, $n = 3$; and P = 0.052, $n = 5$, for MLCKip, wortmannin, and blebbistatin, respectively). Such marginally significant decrease in the SRP size was also observed at 120 s, and occurred regardless of the presence of CaM or inhibitor drugs, indicating nonspecific run-down of the SRP size during WCR (Fig. 4 F, Fig. S7 F, and Table S1).

Summary for the effects of CaM, blebbistatin, and MLCKip on SV pool dynamics

Fig. 5 summarizes the presynaptic effects of CaM, MLCKip, wortmannin, and blebbistatin on the amplitude of $I_{Ca,pre}$ and sizes of the FRP, the SRP, and the total RRP. In Fig. 5 A, we compared baseline values between five presynaptic conditions: addition of DMSO (1/1000, vol/vol; vehicle for blebbistatin as a control, Ctrl), 3 µM CaM (CaM), CaM plus 100 µM blebbistatin (Bleb), CaM plus 10 µM MLCKip (Mip), or CaM plus 3 µM wortmannin (WMN) to the presynaptic pipette solution. The amplitude of $I_{Ca,pre}$, the FRP size, and the total RRP size were not different among all groups (Fig. 5 A, a, b, and d), but the SRP size of Bleb was marginally smaller than that of Ctrl (P = 0.04, *t* test) (Fig. 5 A, c). Inhibition of basal activity of myosin II may reduce preferentially the SRP size. Next, we compared the ratio of an estimate at 40 s after HFS to that before HFS (PTP/Ctrl) for the

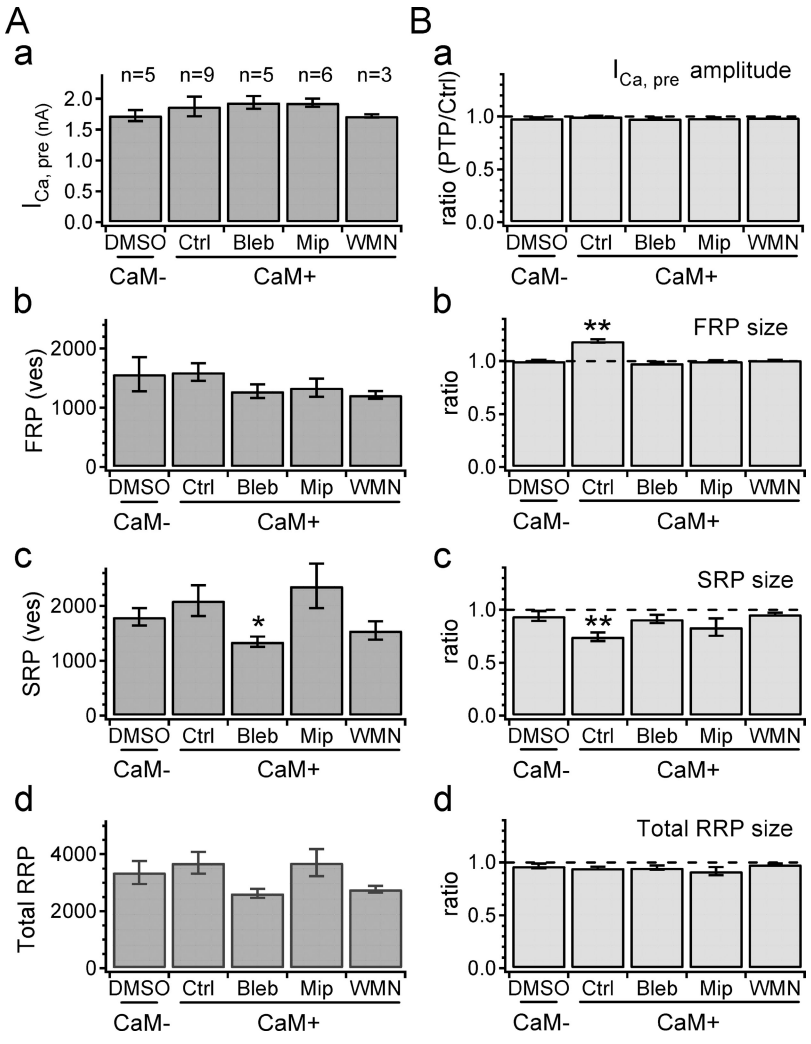

Figure 5. Summary for $I_{Ca,pre}$ amplitude and SV pool sizes before and after HFS (40 s) under different presynaptic conditions. (A) Baseline amplitudes of $I_{Ca,pre}$ and RRP sizes estimated before HFS are compared between different presynaptic conditions: addition of DMSO (DMSO), 3 µM CaM (CaM), CaM plus 100 µM blebbistatin (Bleb), CaM plus 10 µM MLCK inhibitor peptide-18 (Mip) or CaM plus 3 µM wortmannin (WMN) to the presynaptic patch pipette. Mean values for the amplitude of $I_{Ca,pre}$ (a), the FRP size (b), the SRP size (c), and the total RRP size (d) are shown as bar graphs. (B) Ratios of the same parameters as shown in A at 40 s after HFS (PTP) to those before HFS (Ctrl). Mean values for ratio of the amplitudes of $I_{Ca,pre}$ (a), the FRP size (b), the SRP size (c), and the total RRP size (d) are shown. Mean ± SEM, * P < 0.05; ** P < 0.01 (unpaired *t* test).

same set of parameters as in Fig. 5 A. Fig. 5 B demonstrates that the post-tetanic increase of the FRP size accompanies the opposite change of the SRP size when CaM was included in the presynaptic pipette ($n = 9$; Fig. 5 B, b and c), and both changes were inhibited by MLCKip or blebbistatin, implying that the post-tetanic increase in the FRP size may be coupled with the decrease in the SRP size.

A single depolarization pulse for 100 ms induces a change in the FRP size similar to HFS

Given that the activation of MLCK by the $[Ca^{2+}]_{pre}$ elevation during HFS is responsible for the increase in the RRP_{cum} size (Lee et al., 2008), a single long depolarization should be able to substitute for the HFS. To test this hypothesis, we monitored EPSCs after a conditioning pulse of a single depolarization to 0 mV of 50-ms or 100-ms duration. While a 50-ms depolarization pulse induced no change in the FRP size (Fig. S8), a 100-ms depolarization pulse significantly increased the EPSC amplitude observed at 40 s after the conditioning pulse (from 20.1 ± 3.1 nA to 21.6 ± 3.4 nA, $n = 6$, P = 0.01, paired t test). The EPSC amplitude returned to the control value at 120 s (P = 0.39; Fig. 6, B and D). Similar to HFS, the decay τ of EPSC became significantly faster at 40 s after the conditioning pulse (from 23.3 ± 3.2 ms to 21.6 ± 3.0 ms, $n = 6$, $P < 0.01$, paired t test), and returned to the control value at 120 s (P = 0.44; Fig. 6, B and E). The 100-ms conditioning pulse induced a transient increase in the FRP size by 17% at 40 s (from 1492 ± 213 to 1739 ± 230 ves, $n = 6$, $P < 0.01$, paired t test). The FRP size at 120 s was not different from the control value (P = 0.58; Fig. 6 F). Concomitant reduction of the SRP size was observed at 40 s after a 100-ms depolarization pulse (from 2639 ± 267 ves to 2378 ± 253, $n = 6$, $P < 0.01$, paired t test), and the SRP size returned to the control at 120 s (P = 0.10; Fig. 6 G). The total RRP size was not different at all time points (P = 0.73, 40 s, and 0.11, 120 s, $n = 6$; Fig. 6 I). The amplitude of calcium current, the fast and slow release τ at 40 s and at 120 s after conditioning pulse were not significantly different from control values ($n = 6$; Fig. 6 H). These results indicate that presynaptic high Ca^{2+} transient, regardless of how it is delivered, is memorized in the presynaptic terminal as an increase in the FRP size at the expense of the SRP size.

Post-tetanic changes in SV pool is distinct from the effects of ML-9 on the baseline EPSC

Srinivasan et al. (2008) showed that MLCK inhibitors ML-9, ML-7, and wortmannin potentiate the baseline amplitude of EPSC at mice calyx of Held synapses by the mechanism of an increase in the FRP size, which results in the high-frequency EPSC response highly similar to that observed in the present study (Fig. 1 B, c). We tested whether the findings of Srinivasan et al. (2008) are reproduced in the rat calyx of Held synapse. Bath application of 20 µM ML-9 for ∼15 min caused a twofold increase in the amplitude of EPSCs evoked by AFS in the presence of 1 mM kynurenate (Fig. 7 A, a, increase by 106.8 ± 28.8%, $n = 5$, $P < 0.01$, paired t test). Although the effect was weaker than ML-9, ML-7 had a qualitatively similar effect on the baseline amplitude of EPSCs evoked by AFS (Fig. 7 A, b; increase by 28.8 ± 4.5%, $n = 5$, P = 0.049). Distinct from the results in Srinivasan et al. (2008), however, ML-7 and ML-9 potentiated not only the amplitude of early EPSCs but also late steady-state EPSCs evoked by AFS at 100 Hz (Fig. 7, B and C) (see also Fig. 5 A in Lee et al., 2008).

When 3 µM CaM plus 20 µM ML-7 were included in the presynaptic patch pipette, rather higher potentiation of EPSC was observed under dual patch conditions. The amplitude of EPSC (evoked by 50-ms depolarization) was significantly larger than CaM only (36.7 ± 3.5 nA, $n = 4$, vs. 18.75 ± 2.0 nA, $n = 9$, $P < 0.01$, Fig. 7 D) with no significant effect on presynaptic calcium current. Deconvolution analysis of EPSCs evoked by a 50-ms depolarizing pulse revealed that not only the FRP size but also the SRP size were significantly larger in the presence of ML-7 plus CaM compared with CaM only (Fig. 7 D, c; FRP, 3343 ± 380 ves, $n = 4$, $P < 0.01$; SRP, 3539 ± 356 ves, $n = 4$, $P < 0.01$). The effect of ML-7 is in contrast to the post-tetanic changes of SV pool, an increase in the FRP size in parallel with a decrease in the SRP size, indicating that PTP involves a distinct mechanism from the effects of ML-7 on the baseline EPSC. In contrast to the effects of ML-7 and ML-9, intracellular perfusion of wortmannin (5 µM) via presynaptic patch pipette did not significantly affect the baseline EPSC evoked by a 50-ms depolarizing pulse ($n = 4$, P = 0.074; Fig. 7 D). Under dual WCR conditions, bath application of wortmannin (5 µM) did not affect the baseline EPSC either (Fig. 7 D, d). Another MLCK inhibitor, MLCKip, caused nonsignificant reduction of the baseline amplitude of EPSCs evoked by a 50-ms depolarizing pulse under dual WCR conditions (Table S1; $n = 6$, P = 0.45), indicating that the intracellular MLCK inhibitors wortmannin and MLCKip have no consistent effect on the baseline EPSC at least in the rat calyx of Held synapse. The divergence between Srinivasan et al. (2008) and our results may be caused by differences in the species (mouse or rat), and/or in experimental conditions such as presynaptic WCR and supplement of CaM.

DISCUSSION

In the present study we confirmed our previous findings that P_r and the RRP size are differentially regulated during PTP and that CaM-dependent activation of MLCK mediates post-tetanic increase of the RRP_{cum} size (Lee et al., 2008). Rigorous study on the nature of the post-tetanic change in the RRP_{cum} size was hindered because of little PTP under dual WCR conditions (Korogod et al., 2005).

We circumvented the hurdle by including CaM in the presynaptic pipette solution. Presynaptic supplement of CaM rescued the post-tetanic increase in the RRP_{cum} size, but not the increase in P_r. These findings are in agreement with our previous result that a mechanism involving CaM is responsible only for the post-tetanic

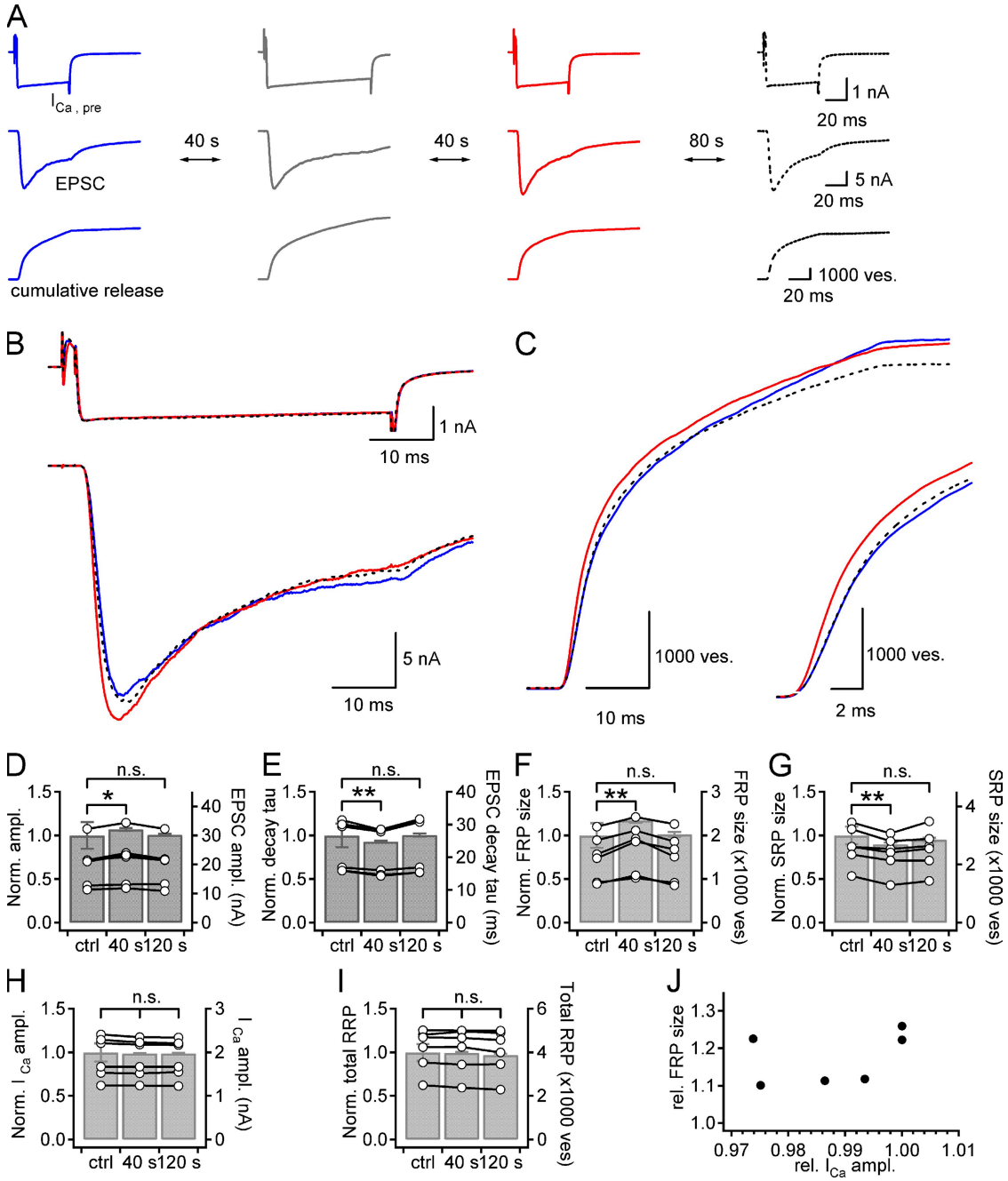

Figure 6. A transient increase in the FRP size can be induced by a single conditioning pulse. (A) Experimental protocol is the same as in Fig. 2 except that a train of AP-like pulses were replaced with a single depolarization pulse to 0 mV for 100 ms duration (conditioning pulse, second column). Presynaptic Ca^{2+} current ($I_{Ca,pre}$, top), EPSC (middle), and cumulative release (bottom) are shown in a sequential order. (B and C) Presynaptic Ca^{2+} current (B, top), EPSCs (B, bottom), and cumulative quantal release (C). Each panel shows three superimposed traces recorded at the same synapse as in A at the 40 s before (blue solid line) and 40 s (red solid line) and 120 s (broken line) after the conditioning pulse. (C, inset) A trace for the cumulative release on an expanded time scale. (D–I) Statistical mean of relative values before (ctrl) and after HFS (40 s and 120 s) normalized to the control value measured before HFS. (D) EPSC amplitude; (E) decaying time constant of EPSC; (F) size of the FRP; (G) size of the SRP; (H) the amplitude of $I_{Ca,pre}$; (I) size of the total RRP. Data of individual synapses are shown as circles connected with a line (right ordinate). Error bar, SEM; *, $P < 0.05$; **, $P < 0.01$; n.s., not significant ($P > 0.05$, paired *t* test). (J) Relative FRP sizes as a function of relative amplitudes of $I_{Ca,pre}$ at 40 s after conditioning ($n = 6$). Each point of data was normalized to the value measured before applying a conditioning pulse.

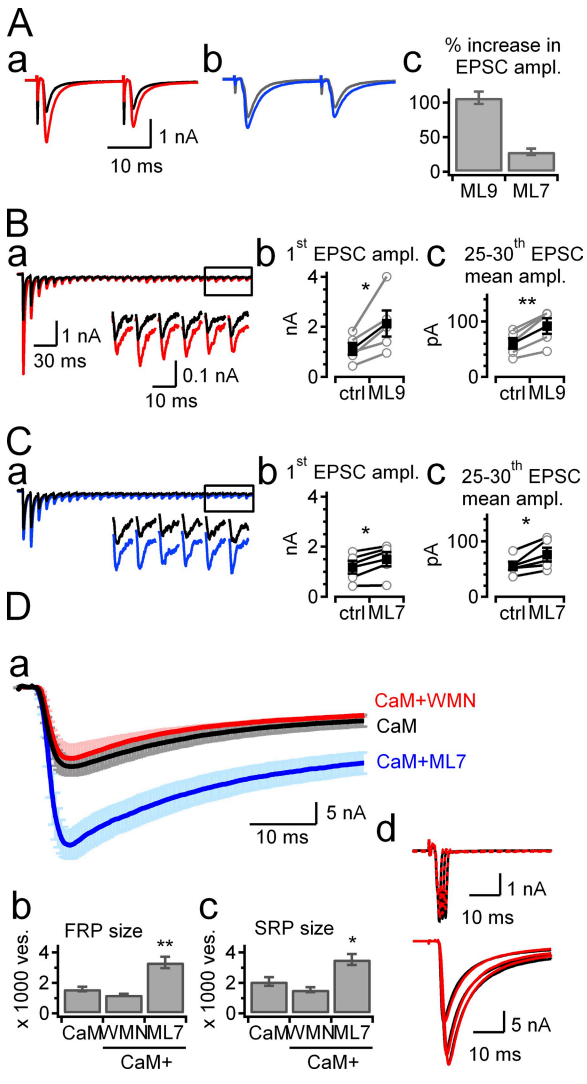

Figure 7. The effects of MLCK inhibitors on the baseline synaptic transmission. (A, a and b) Representative EPSCs evoked by a paired pulse stimulation (ISI, 20 ms) of afferent fibers at 0.1 Hz in the presence of 1 mM kynurenate. EPSCs recorded under control conditions (black) and in the presence of ML-9 (20 μM, A, a, red) or ML-7 (20 μM, A, b, blue) are superimposed. (A, c) Percentage change in baseline amplitude of EPSC on application of ML-9 ($n = 4$) or ML7 ($n = 5$). (B, a, and C, a) Train of EPSCs (30 pulses at 100 Hz) under control conditions (black) and after bath application of ML9 (B, a, red) or ML-7 (C, a, blue) are superimposed. Inset, enlarged last six EPSCs. Summary graph for the peak amplitude of first EPSC (B, b, and C, b) and for the mean peak amplitude of last 6 EPSCs (B, c, and C, c) under control conditions (ctrl) and in the presence of ML-9 (B) or ML-7 (C). (D, a) EPSCs were evoked by presynaptic step depolarization to 0 mV for 50 ms duration preceded by +70 mV for 2-ms predepolarizing pulse using presynaptic patch pipette containing CaM only (3 μM, black), CaM plus wortmannin (5 μM, red), or CaM plus ML7 (20 μM, blue). EPSCs obtained from different synapses under each intracellular condition were averaged, and the averaged traces are superimposed with error bars (light colored). (D, b and c) Summary graphs for mean sizes of FRP (D, b) and SRP (D, c) estimated from deconvolution analysis of EPSCs evoked by a 50-ms depolarizing pulse with CaM only (CaM), CaM plus wortmannin (WMN), or CaM plus ML-7 (ML7) included in the presynaptic pipette. (D, d) Presynaptic calcium currents (top) and concomitant EPSCs (bottom) evoked by presynaptic depolarization to 0 mV for 1, 2, and 3 ms in duration. Traces under control conditions (black) and those recorded at 5 min after bath application of 5 μM wortmannin are superimposed (red). Presynaptic patch pipette contained 3 μM CaM.

change in the RRP_{cum} size. The present study extended our previous findings by showing that the total RRP size does not increase during PTP, and that it is the proportion of the FRP and the SRP sizes that undergoes the post-tetanic modulation. Given that the FRP is a major contributor to the RRP_{cum} size (Sakaba, 2006), the post-tetanic increases in the RRP_{cum} size and in the ratio of FRP to SRP sizes seem to share the common mechanism. Supporting this idea, both post-tetanic changes were not observed without presynaptic supplement of CaM and were suppressed by the inhibitor of myosin II or MLCK. Furthermore, the opposite changes in FRP and SRP sizes during PTP provide compelling evidence for conversion of a slowly releasing SV into a rapidly releasing SV, which has been hypothesized by Neher and Sakaba (2008). Therefore, the present study elucidated a new physiological role of slowly releasing SVs, which has been considered to play a role only in asynchronous release (Sakaba, 2006).

The shift of SVs from SRP to FRP is a novel mechanism for short-term plasticity

The CaM-dependent post-tetanic effects observed in the present study are clearly different from the effects of phorbol esters or residual calcium-dependent enhancement of EPSC, because neither of them changed the EPSC amplitude evoked by maximal depolarization with long duration (>20 ms). Instead, they enhanced EPSC evoked by a presynaptic spike or submaximal short depolarization, which is interpreted as an increase in P_r (Felmy et al., 2003; Awatramani et al., 2005; Lou et al., 2008). We measured the residual calcium level at 40 s after HFS under dual WCR conditions and found that $\Delta[Ca^{2+}]_i$ was <10 nM in most synapses (Fig. 3 D). Moreover, post-tetanic modulation of the RRP was not observed in the absence of CaM, which may not affect residual calcium. Our previous results also demonstrated that activation of PKC is not responsible for PTP induced by HFS at 100 Hz for 4 s (but see Korogod et al., 2007). These observations argue against residual calcium or activation of PKC as a mechanism for the post-tetanic effects on the RRP. The post-tetanic increase in the FRP size is also distinct from that induced by cAMP, because the latter has no effect on the SRP size resulting in an increase in the total RRP size (Sakaba and Neher, 2001b). Therefore, the CaM and MLCK-mediated increase in the proportion of FRP to SRP is a novel mechanism for short-term synaptic plasticity.

Fusion-competent SVs in the RRP can be separated into two components (FRP and SRP) according to their release kinetics by 0.5 mM EGTA in the presynaptic pipette. Both molecular fusion competence and the proximity of SV to a calcium source have been suggested to determine the release kinetics of a given SV, although it is controversial, which is a primary factor (Wadel et al., 2007; Wolfel et al., 2007). The present study showed that the proportion of the FRP to the total RRP was transiently enhanced by a mechanism involving myosin II and MLCK, while total RRP size was kept unchanged. It has been demonstrated that inhibition of MLCK slows down vesicle mobility in intact synaptic boutons (Jordan et al., 2005). In addition, MLCK might alter the interaction of docked SV with nearby Ca^{2+} channels (Srinivasan et al., 2008). Assuming that myosin plays a role in translocation of SV, results of the present study imply that myosin may help an SV to be matured by translocation of SVs close to a calcium source (so-called "positional priming") (Neher and Sakaba, 2008; Fig. 8). Therefore, the size of the FRP may not be static but in dynamic equilibrium with the SRP, and the equilibrium can be shifted toward FRP by Ca^{2+}/CaM-dependent activation of MLCK.

CaM-binding motifs in presynaptic proteins

The finding that CaM required for the post-tetanic increase in the FRP can be washed out by presynaptic WCR suggests that CaM is not constitutively bound to the effector molecule, probably MLCK. Consistent with this notion, the half-maximal $[Ca^{2+}]$ for binding of CaM to nonmuscle MLCK is fairly high (probably higher than 1 µM; Peersen et al., 1997), and thus CaM bound to MLCK should be negligible at resting $[Ca^{2+}]_i$, especially when 0.5 mM EGTA is included in the presynaptic pipette solution. Supplemental CaM may not be required for observation of a biological process that involves Ca^{2+}-independent, CaM-binding motif. This may be the case when low $[Ca^{2+}]$ is sufficient for binding of CaM to an effector molecule such as Munc13-2 (EC_{50} = 100 nM; Zikich et al., 2008). This may explain why CaM-dependent recovery of the FRP could be observed at the calyx of Held without supplement of CaM (Sakaba and Neher, 2001a; Hosoi et al., 2007).

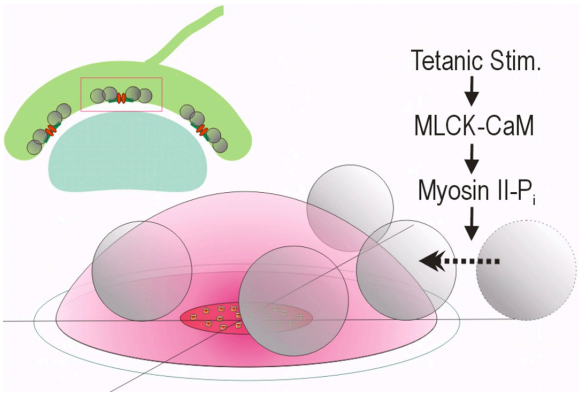

Figure 8. Conceptual diagram for the post-tetanic transient increase in the FRP size in a calyx of Held. The diagram shows a schematic model for an active zone in a calyx of Held (red box, inset), which consists of a cluster of calcium channels at the center and four docked SVs (gray spheres) with variable distance from the calcium source (Meinrenken et al. 2002). It is assumed that the proximity of a SV to the Ca^{2+} source (positional priming) is a primary determinant of release kinetics of the SV, and thus two docked SVs which belong to an FRP reside inside the calcium microdomain (red dome), while the rest (two SVs in an SRP) resides outside the microdomain. Results of the present and our previous studies (Lee et al., 2008) imply that presynaptic Ca^{2+} elevation in the presence of CaM during tetanic stimulation activates MLCK and then myosin II, which in turn facilitates translocation of slowly releasing SVs toward the Ca^{2+} source. The alternative possibility that MLCK may facilitate the final step of molecular priming is not illustrated.

Post-tetanic changes in releasing time constants and the amplitude of mEPSC

Releasing time constants of the FRP (τ_{fast}) in three conditions of presynaptic treatment with 3 µM CaM (CaM, CaM + blebbistatin, CaM + wortmannin) were significantly slower than that in the CaM-free conditions (DMSO, $P \leq 0.01$) (Fig. S9 A). A calcium-buffering effect of CaM may be responsible for the retardation of fast release kinetics, because CaM, which has four calcium-binding motifs can retard the spatial expansion of calcium microdomain at the beginning of depolarization. Although presynaptic CaM slowed the baseline τ_{fast}, the post-tetanic retardation of τ_{fast} was observed only in the absence of CaM (Fig. 2 J and Fig. S5 J). Without CaM, τ_{fast} slowed by 23.8% on average after HFS (n = 5) (Fig. S9 B). The mechanism underlying CaM-dependent regulation of τ_{fast} remains to be elucidated. Presynaptic supplement of CaM may facilitate the recovery of τ_{fast} after HFS. Alternatively, slower baseline τ_{fast} in the presence of CaM may occlude the post-tetanic increase of τ_{fast}.

Recently, it has been reported that presynaptic long depolarization induces an increase of the quantal size in a Ca^{2+}- and synaptotagmin2-dependent manner (He et al., 2009). A distinct increase in the quantal size required fairly long duration of HFS. Whereas 10% increase in the mean amplitude of mEPSC has been reported at 100 Hz for 4 s (He et al., 2009), Korogod et al. (2005) observed no difference in the distribution of mEPSC amplitudes, suggesting that HFS at 100 Hz for 4 s is an ambiguous condition for inducing a robust increase in quantal size. Under our experimental conditions (0.5 mM EGTA), no difference was found before and after HFS (100 Hz for 4 s), probably due to higher calcium buffer concentration (Fig. S3). Therefore, the increase in the FRP size cannot be ascribed to the change in the quantal size. Second, it has been reported that an increase in Ca^{2+} influx contributes to the increase in P_r during PTP at the calyx of Held synapse

(Habets and Borst, 2006). We observed, however, no consistent post-tetanic change of Ca^{2+} current. In some terminals (three of nine cells in Fig. 2 L) that were supplemented with CaM, presynaptic Ca^{2+} current increased by up to 2.9% at 40 s after HFS, but no increase in $I_{Ca,pre}$ was observed in other terminals. Probably, post-tetanic increase in $I_{Ca,pre}$ may require a diffusible Ca^{2+} sensor molecule other than CaM such as NCS-1 (Tsujimoto et al., 2002; Habets and Borst, 2006).

Temperature-dependence of PTP

Synaptic transmission and vesicle recruitment rates are strongly dependent on temperature (Kushmerick et al., 2006). Because the post-tetanic increase in P_r decays faster at physiological temperature (PT) than at RT, the increase in P_r is restricted to the augmentation phase, and thereby an increase in the RRP size dominates PTP at PT (Habets and Borst, 2007). Similar transient increase in the RRP size has been observed during the recovery time course after a depleting pulse at PT, but not at RT, in chromaffin cells, and the overfill of the RRP was closely associated with a temperature-dependent acceleration of the recovery of RRP (Dinkelacker et al., 2000). At the calyx of Held synapse, the recovery rate of RRP was enhanced at PT, but an overshoot in the RRP size did not occur (Kushmerick et al., 2006). To test whether the recovery is accelerated during PTP, we studied the recovered fraction of FRP at 750 ms after depleting pulse (50 ms) before and 40 s after HFS, and found no significant acceleration of the recovery (unpublished data), suggesting that enhanced refilling rate is not involved in the post-tetanic transient increase in the FRP size.

Relevance of the post-tetanic RRP changes to glutamatergic synaptic transmission

Not only the calyx of Held but also small glutamatergic synapse terminals exhibit a disparity between the RRP_{cum} size and the size of total releasable vesicle pools, which can be measured by presynaptic long depolarization or hypertonic sucrose (Moulder and Mennerick, 2005). Given that SVs that are not depleted by HFS comprise an SV pool analogous to SRP at the calyx of Held, it is plausible that post-tetanic increase in the FRP could be a mechanism for PTP at small glutamatergic synapses. Recently, it has been suggested that short-term enhancement of synaptic efficacy, which can be implemented by presynaptic residual calcium, may be an energetically less expensive neural substrate for working memory in comparison with a persistent reverberation (Mongillo et al., 2008). It has been shown that residual calcium and post-tetanic increase in the RRP_{cum} size constitute fast and slow components of the biphasic decay of PTP, respectively (Habets and Borst, 2007; Lee et al., 2008). Therefore, it remains to be elucidated whether the post-tetanic transient increase in the FRP size can be used as a memory buffer that lasts longer than residual calcium for maintaining working memory.

This research was supported by a grant (2009K001247) from Brain Research Center of the 21st Century Frontier Research Program funded by the Ministry of Science and Technology, the Republic of Korea. J. S. Lee is a postgraduate student supported by Program BK21 from the Ministry of Education.

Edward N. Pugh, Jr. served as editor.

Submitted: 22 March 2010
Accepted: 02 July 2010

REFERENCES

Awatramani, G.B., G.D. Price, and L.O. Trussell. 2005. Modulation of transmitter release by presynaptic resting potential and background calcium levels. *Neuron.* 48:109–121. doi:10.1016/j.neuron.2005.08.038

Borst, J.G., and B. Sakmann. 1996. Calcium influx and transmitter release in a fast CNS synapse. *Nature.* 383:431–434. doi:10.1038/383431a0

Dinkelacker, V., T. Voets, E. Neher, and T. Moser. 2000. The readily releasable pool of vesicles in chromaffin cells is replenished in a temperature-dependent manner and transiently overfills at 37°C. *J. Neurosci.* 20:8377–8383.

Felmy, F., E. Neher, and R. Schneggenburger. 2003. Probing the intracellular calcium sensitivity of transmitter release during synaptic facilitation. *Neuron.* 37:801–811. doi:10.1016/S0896-6273(03)00085-0

Habets, R.L., and J.G. Borst. 2005. Post-tetanic potentiation in the rat calyx of Held synapse. *J. Physiol.* 564:173–187. doi:10.1113/jphysiol.2004.079160

Habets, R.L., and J.G. Borst. 2006. An increase in calcium influx contributes to post-tetanic potentiation at the rat calyx of Held synapse. *J. Neurophysiol.* 96:2868–2876. doi:10.1152/jn.00427.2006

Habets, R.L., and J.G. Borst. 2007. Dynamics of the readily releasable pool during post-tetanic potentiation in the rat calyx of Held synapse. *J. Physiol.* 581:467–478. doi:10.1113/jphysiol.2006.127365

He, L., L. Xue, J. Xu, B.D. McNeil, L. Bai, E. Melicoff, R. Adachi, and L.G. Wu. 2009. Compound vesicle fusion increases quantal size and potentiates synaptic transmission. *Nature.* 459:93–97. doi:10.1038/nature07860

Hosoi, N., T. Sakaba, and E. Neher. 2007. Quantitative analysis of calcium-dependent vesicle recruitment and its functional role at the calyx of Held synapse. *J. Neurosci.* 27:14286–14298. doi:10.1523/JNEUROSCI.4122-07.2007

Jordan, R., E.A. Lemke, and J. Klingauf. 2005. Visualization of synaptic vesicle movement in intact synaptic boutons using fluorescence fluctuation spectroscopy. *Biophys. J.* 89:2091–2102. doi:10.1529/biophysj.105.061663

Kim, M.H., N. Korogod, R. Schneggenburger, W.K. Ho, and S.H. Lee. 2005. Interplay between Na+/Ca2+ exchangers and mitochondria in Ca2+ clearance at the calyx of Held. *J. Neurosci.* 25:6057–6065. doi:10.1523/JNEUROSCI.0454-05.2005

Korogod, N., X. Lou, and R. Schneggenburger. 2005. Presynaptic Ca2+ requirements and developmental regulation of posttetanic potentiation at the calyx of Held. *J. Neurosci.* 25:5127–5137. doi:10.1523/JNEUROSCI.1295-05.2005

Korogod, N., X. Lou, and R. Schneggenburger. 2007. Posttetanic potentiation critically depends on an enhanced Ca2+ sensitivity of vesicle fusion mediated by presynaptic PKC. *Proc. Natl. Acad. Sci. USA.* 104:15923–15928. doi:10.1073/pnas.0704603104

Kushmerick, C., R. Renden, and H. von Gersdorff. 2006. Physiological temperatures reduce the rate of vesicle pool depletion and

short-term depression via an acceleration of vesicle recruitment. *J. Neurosci.* 26:1366–1377. doi:10.1523/JNEUROSCI.3889-05.2006

Lee, J.S., M.-H. Kim, W.-K. Ho, and S.-H. Lee. 2008. Presynaptic release probability and readily releasable pool size are regulated by two independent mechanisms during posttetanic potentiation at the calyx of Held synapse. *J. Neurosci.* 28:7945–7953. doi:10.1523/JNEUROSCI.2165-08.2008

Lou, X., N. Korogod, N. Brose, and R. Schneggenburger. 2008. Phorbol esters modulate spontaneous and Ca2+-evoked transmitter release via acting on both Munc13 and protein kinase C. *J. Neurosci.* 28:8257–8267. doi:10.1523/JNEUROSCI.0550-08.2008

Meinrenken, C.J., J.G.G. Borst, and B. Sakmann. 2002. Calcium secretion coupling at calyx of Held governed by nonuniform channel–vesicle topography. *J. Neurosci.* 22:1648–1667.

Mongillo, G., O. Barak, and M. Tsodyks. 2008. Synaptic theory of working memory. *Science.* 319:1543–1546. doi:10.1126/science.1150769

Moulder, K.L., and S. Mennerick. 2005. Reluctant vesicles contribute to the total readily releasable pool in glutamatergic hippocampal neurons. *J. Neurosci.* 25:3842–3850. doi:10.1523/JNEUROSCI.5231-04.2005

Neher, E., and T. Sakaba. 2001. Combining deconvolution and noise analysis for the estimation of transmitter release rates at the calyx of Held. *J. Neurosci.* 21:444–461.

Neher, E., and T. Sakaba. 2008. Multiple roles of calcium ions in the regulation of neurotransmitter release. *Neuron.* 59:861–872. doi:10.1016/j.neuron.2008.08.019

Peersen, O.B., T.S. Madsen, and J.J. Falke. 1997. Intermolecular tuning of calmodulin by target peptides and proteins: differential effects on Ca2+ binding and implications for kinase activation. *Protein Sci.* 6:794–807. doi:10.1002/pro.5560060406

Pusch, M., and E. Neher. 1988. Rates of diffusional exchange between small cells and a measuring patch pipette. *Pflugers Arch.* 411:204–211. doi:10.1007/BF00582316

Sakaba, T. 2006. Roles of the fast-releasing and slowly releasing vesicles in synaptic transmission at the calyx of Held. *J. Neurosci.* 26:5863–5871. doi:10.1523/JNEUROSCI.0182-06.2006

Sakaba, T., and E. Neher. 2001a. Calmodulin mediates rapid recruitment of fast-releasing synaptic vesicles at a calyx-type synapse. *Neuron.* 32:1119–1131. doi:10.1016/S0896-6273(01)00543-8

Sakaba, T., and E. Neher. 2001b. Preferential potentiation of fast-releasing synaptic vesicles by cAMP at the calyx of Held. *Proc. Natl. Acad. Sci. USA.* 98:331–336. doi:10.1073/pnas.021541098

Sätzler, K., L.F. Sohl, J.H. Bollmann, J.G.G. Borst, M. Frotscher, B. Sakmann, and J.H.R. Lubke. 2002. Three-dimensional reconstruction of a calyx of Held and its postsynaptic principal neuron in the medial nucleus of the trapezoid body. *J. Neurosci.* 22:10567–10579.

Schneggenburger, R., T. Sakaba, and E. Neher. 2002. Vesicle pools and short-term synaptic depression: lessons from a large synapse. *Trends Neurosci.* 25:206–212. doi:10.1016/S0166-2236(02)02139-2

Srinivasan, G., J.H. Kim, and H. von Gersdorff. 2008. The pool of fast releasing vesicles is augmented by myosin light chain kinase inhibition at the calyx of Held synapse. *J. Neurophysiol.* 99:1810–1824. doi:10.1152/jn.00949.2007

Tokuoka, H., and Y. Goda. 2006. Myosin light chain kinase is not a regulator of synaptic vesicle trafficking during repetitive exocytosis in cultured hippocampal neurons. *J. Neurosci.* 26:11606–11614. doi:10.1523/JNEUROSCI.3400-06.2006

Tsujimoto, T., A. Jeromin, N. Saitoh, J.C. Roder, and T. Takahashi. 2002. Neuronal calcium sensor 1 and activity-dependent facilitation of P/Q-type calcium currents at presynaptic nerve terminals. *Science.* 295:2276–2279. doi:10.1126/science.1068278

Wadel, K., E. Neher, and T. Sakaba. 2007. The coupling between synaptic vesicles and Ca2+ channels determines fast neurotransmitter release. *Neuron.* 53:563–575. doi:10.1016/j.neuron.2007.01.021

Wolfel, M., X. Lou, and R. Schneggenburger. 2007. A mechanism intrinsic to the vesicle fusion machinery determines fast and slow transmitter release at a large CNS synapse. *J. Neurosci.* 27:3198–3210. doi:10.1523/JNEUROSCI.4471-06.2007

Wu, L.G., and J.G. Borst. 1999. The reduced release probability of releasable vesicles during recovery from short-term synaptic depression. *Neuron.* 23:821–832. doi:10.1016/S0896-6273(01)80039-8

Zikich, D., A. Mezer, F. Varoqueaux, A. Sheinin, H.J. Junge, E. Nachliel, R. Melamed, N. Brose, M. Gutman, and U. Ashery. 2008. Vesicle priming and recruitment by ubMunc13-2 are differentially regulated by calcium and calmodulin. *J. Neurosci.* 28:1949–1960. doi:10.1523/JNEUROSCI.5096-07.2008